Example of a Physical System with a Hyperbolic Attractor of the Smale-Williams Type

Sergey P. Kuznetsov

Institute of Radio-Engineeing and Electronics of RAS, Saratov Division, Zelenaya 38 Saratov, 410019, Russia

(Received 18 March 2005; published 28 September 2005)

A simple and transparent example of a nonautonomous flow system with a hyperbolic strange attractor is suggested. The system is constructed on the basis of two coupled van der Pol oscillators, the characteristic frequencies differ twice, and the parameters controlling generation in both oscillators undergo a slow periodic counterphase variation in time. In terms of stroboscopic Poincaré sections, the respective 4D mapping has a hyperbolic strange attractor of the Smale-Williams type. Qualitative reasoning and quantitative data of numerical computations are presented and discussed, e.g., Lyapunov exponents and their parameter dependencies. A special test for hyperbolicity based on analysis of distributions of angles between stable and unstable subspaces of a chaotic trajectory is performed.

DOI: 10.1103/PhysRevLett.95.144101 PACS numbers: 05.45.−a, 05.40.Ca

Mathematical theory of chaotic dynamics based on a rigorous axiomatic foundation exploits a notion of hyperbolicity, which implies that all relevant trajectories in phase space of a system are of saddle type, with well-defined stable and unstable directions [1–4]. Dissipative hyperbolic systems contracting the phase space volume manifest robust strange attractors with strong chaotic properties. The robustness (structural stability) [1,2,5] implies insensitivity of the motions with respect to variations of dynamical equations. In particular, Cantor-like structure of the hyperbolic strange attractor persists without qualitative changes (bifurcations), at least while the variations are not too large. The largest Lyapunov exponent depends on parameters in smooth manner. Textbook examples of these robust strange attractors are artificial mathematical constructions associated with discrete-time models, e.g., the Plykin attractor and Smale-Williams solenoid.

It seems that the mathematical theory of hyperbolic chaos has never been applied conclusively to any physical object, although concepts of this theory are widely used for interpretation of chaotic behavior of realistic nonlinear systems. On the other hand, feasible nonlinear systems with complex dynamics, such as chaotic self-oscillators, driven nonlinear oscillators, Rössler model, etc., do not relate to the true hyperbolic class [4,6,7]. As a rule, observable chaos in these systems is linked with a so-called quasiattractor, on which chaotic trajectories coexist with stable orbits of high periods (usually indistinguishable in computations at reasonable accuracies). A mathematical description of quasiattractors remains a challenging problem, although in physical systems the nonhyperbolicity is masked effectively due to presence of noise. In a few cases, e.g., in Lorenz model in some appropriate domain of the parameter space, dynamics is proved to be quasihyperbolic (with restrictions concerning violation of axiomatic statements of hyperbolicity in some detail) [8,9].

I am aware of a few works which discuss examples of true hyperbolic dynamics in systems governed by differential equations. One relates to a system called triple linkage, which allows description in terms of motion on a surface of negative curvature in a frictionless case. In the presence of dissipation and feedback, it is expected to manifest a hyperbolic chaotic attractor [10]. In Ref. [11] the author constructs an artificial 3D flow system possessing an attractor of Plykin type in the Poincaré map. This example definitely looks too complicated to be realizable as a physical device. Finally, in Ref. [12] the authors argue in favor of the existence of an attractor of Plykin type in a 3D flow system motivated by neural dynamics.

In this Letter, I suggest a simple and transparent example of a nonautonomous flow system, which apparently manifests a hyperbolic strange attractor. In terms of stroboscopic Poincaré map, it is an attractor of the same kind as the Smale-Williams solenoid, but embedded in a 4D rather than 3D state space. This system, for sure, may be designed, e.g., as an electronic device [13].

The system is constructed on the basis of two van der Pol oscillators with characteristic frequencies ω_0 and $2\omega_0$. The control parameters responsible for the Andronov-Hopf bifurcations in the subsystems are forced to swing slowly, periodically in time. On a half-period, the first oscillator is excited and the second one remains below the generation threshold. On another half-period the situation is the opposite. Next, we assume that the first oscillator acts on the partner via a quadratic term in the equation. The produced second harmonic component serves as a primer for the second oscillator, as it comes off the under-threshold state. In turn, the second oscillator acts on the first one via a term represented by a product of the dynamical variable and an auxiliary signal of frequency ω_0. Thus, a component with the difference frequency appears, which fits the resonance range for the first oscillator and serves as a primer as it starts to generate.

Summarizing this description, we write down the following equations:

$$\begin{aligned} &\ddot{x} - (A\cos 2\pi t/T - x^2)\dot{x} + \omega_0^2 x = \varepsilon y \cos\omega_0 t, \\ &\ddot{y} - (-A\cos 2\pi t/T - y^2)\dot{y} + 4\omega_0^2 y = \varepsilon x^2, \end{aligned} \tag{1}$$

where x and y are dynamical variables of the first and the

second oscillator, respectively, A is a constant designating amplitude of the slow swing of the parameters, and ε is a coupling parameter.

We assume that the period of swing T contains an integer number of periods of the auxiliary signal: $T = 2\pi N/\omega_0$. Thus, our set of nonautonomous equations has periodic coefficients, and it is appropriate to treat the dynamics in terms of stroboscopic Poincaré section.

Let us suppose that we have an instantaneous state given by a vector $\mathbf{V}_n = \{x, \dot{x}/\omega_0, y, \dot{y}/(2\omega_0)\}$ at $t_n = nT$. Then, after one time interval T we get a new state

$$\mathbf{V}_{n+1} = \mathbf{F}(\mathbf{V}_n). \tag{2}$$

Here $\mathbf{F}$ is some vector function, which acts in a 4D space of vectors $\mathbf{V}$. This procedure defines a Poincaré map for our system and delivers an alternative description of the dynamics in terms of discrete-time steps T [instead of the continuous time description with Eqs. (1)]. Actual construction of the map may be performed by means of numerical solution of Eqs. (1).

To consider operation of the system on a qualitative level, let us assume that on a stage of generation the first oscillator has some phase φ: $x \propto \cos(\omega_0 t + \varphi)$. The squared value x^2 contains the second harmonic: $\cos(2\omega_0 t + 2\varphi)$, and its phase is 2φ. As the half-period comes to an end, and the second oscillator becomes excited, the induced oscillations of the variable y get the same phase 2φ. Mixture of these oscillations with the auxiliary signal transfers the doubled phase into the original frequency range. Hence, on the next stage of excitation the first oscillator accepts this phase 2φ. Obviously, on subsequent stages of swing the phases of the first oscillator follow approximately the mapping

$$\varphi_{n+1} = 2\varphi_n (\mathrm{mod} 2\pi). \tag{3}$$

Figure 1 shows typical time dependence for x and y obtained from numerical solution of Eqs. (1) by the Runge-Kutta method for parameter values $\omega_0 = 2\pi$, $T = N = 10$, $A = 3$, and $\varepsilon = 0.5$ and a plot of empirical map for phase φ_{n+1} versus φ_n. The phases are determined for the first oscillator at time instants $t_n = nT$:

$$\varphi = \begin{cases} \arctan(-\omega_0^{-1}\dot{x}/x), & x > 0, \\ \arctan(-\omega_0^{-1}\dot{x}/x) + \pi, & x < 0. \end{cases} \tag{4}$$

The mapping for the phase looks, as expected, topologically equivalent to the relation (3). (Some distortions arise due to imperfection of the above qualitative considerations and of the definition of phase; the correspondence becomes better at larger N.) The chaotic nature of the dynamics reveals itself in a random walk of humps on subsequent periods of swing in respect to the envelope of the generated signal.

In terms of the stroboscopic Poincaré map (2), attractors of the system correspond exactly to the construction of Smale and Williams. In the 4D state space, the direction associated with the phase φ is expanding and gives rise to a positive Lyapunov exponent of the map $\Lambda_1 \approx \log 2$. Three rest directions are contracting and correspond to a 3D stable manifold of the attractor. Three respective Lyapunov exponents are negative. Interpreting the stroboscopic Poincaré mapping, we may imagine a solid 4D toroid (direct product of a 3D ball and a 1D circle) and associate one iteration of the map with longitudinal stretch, contraction in the transversal directions, and insertion of the doubly folded ''tube'' into the original toroid.

In computations, the Lyapunov exponents were evaluated with a help of Benettin's algorithm [14,15] from simultaneous solution of Eqs. (1) together with a collection of four exemplars of the linearized equations

$$\ddot{\tilde{x}} + 2x\dot{x}\,\tilde{x} - (A\cos 2\pi t/T - x^2)\dot{\tilde{x}} + \omega_0^2\tilde{x} = \varepsilon\tilde{y}\cos\omega_0 t,$$
$$\ddot{\tilde{y}} + 2y\dot{y}\,\tilde{y} - (-A\cos 2\pi t/T - y^2)\dot{\tilde{y}} + 4\omega_0^2\tilde{y} = 2\varepsilon x\tilde{x} \tag{5}$$

for an integer number of periods T. In the course of the solution, at each step of the integration schema, the Gram-Schmidt orthogonalization and normalization were performed for four vectors $\{\tilde{x}(t), \dot{\tilde{x}}(t)/\omega_0, \tilde{y}(t), \dot{\tilde{y}}(t)/2\omega_0\}$, and the mean rates of growth or decrease of the accumulated sums of logarithms of the norms (after the orthogonalization but before the normalization) were estimated. Obviously, four Lyapunov exponents for the differential equations λ_k and for the stroboscopic map Λ_k are linked as $\lambda_k = T^{-1}\Lambda_k$. In particular, for the attractor at the above-mentioned parameters $\lambda_1 \approx 0.068 \approx T^{-1}\log 2$, $\lambda_2 \approx -0.35$, $\lambda_3 \approx -0.59$, and $\lambda_4 \approx -0.81$. (Notice the absence

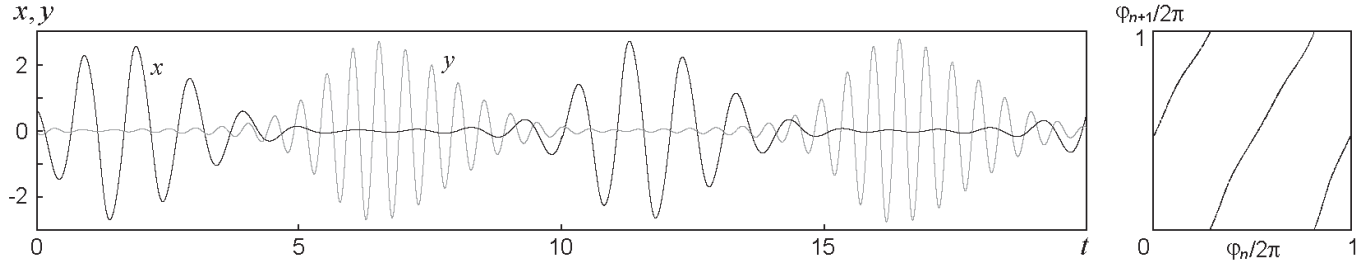

FIG. 1. A typical pattern of time dependence for variables x and y obtained from numerical solution of Eqs. (1) for $\omega_0 = 2\pi$, $T = N = 10$, $A = 3$, and $\varepsilon = 0.5$ (left panel) and a diagram of empirical mapping for phase of the first oscillator defined on stages of excitation at $t_n = nT$ (right panel).

of a zero Lyapunov exponent: this is natural for maps and nonautonomous flow systems.)

If the attractor is indeed hyperbolic, the chaotic dynamics must be robust and retain its character under (at least small) variations of the equations. As checked, this is indeed the case. In particular, as seen from Fig. 2, the largest Lyapunov exponent is almost independent on parameter A, and other exponents manifest rather regular parameter dependences.

Dynamical behavior of the same kind is observed at other integer period ratios, including essentially smaller ones, e.g., $N = 4$. Figure 3 shows a portrait of the strange attractor in the Poincaré section projected onto the plane $(x, \dot{x})$ at $\omega_0 = 2\pi$, $T = N = 4$, $A = 8$, and $\varepsilon = 0.5$. It looks precisely as the Smale-Williams attractor should look. Observe the fractal transversal structure of "strips" constituting the attractor. In this case, the Lyapunov exponents are $\lambda_1 \approx 0.17$, $\lambda_2 \approx -0.66$, $\lambda_3 \approx -1.03$, and $\lambda_4 \approx -1.53$. An estimate for fractal dimension from the Kaplan-Yorke formula [16] yields $D \approx 1.26$, and that from Grassberger-Procaccia algorithm [16,17] is $D \approx 1.26$.

It is interesting to perform a direct numerical test for hyperbolicity of the attractor. The idea for such test was suggested in Refs. [18,19] and applied for verification of hyperbolicity of trajectories of dynamical systems, which have one stable and one unstable direction. The procedure consists of computations of vectors of small perturbations along the trajectory, in forward and in inverse time, measuring angles between the forward-time and backward-time vectors at points on the trajectory. If zero values of the angle do not occur, one concludes that the dynamics is hyperbolic. If the angle distribution shows a nonvanishing probability of angles close to zero, it implies nonhyperbolicity because of the presence of the homoclinic tangencies of stable and unstable manifolds. In dissipative cases these tangencies are responsible for the occurrence of quasiattractors.

In our case the method needs a modification. First, we intend to deal with description in terms of stroboscopic map (2) to link the results directly with the Smale-Williams construction. Second, in our case only unstable subspace is one dimensional, and the stable subspace is three dimensional. An adopted algorithm consists of the following. First, we generate a sufficiently long representative orbit $\{x(t), \dot{x}(t)/\omega_0, y(t), \dot{y}(t)/2\omega_0\}$ on the attractor from the numerical solution of Eqs. (1). Then, we solve numerically the Eqs. (5) forward in time. In the course of the solution, normalization of the vector $\mathbf{a}(t) = \{\tilde{x}(t), \dot{\tilde{x}}(t)/\omega_0, \tilde{y}(t), \dot{\tilde{y}}(t)/2\omega_0\}$ is performed at each step of integration to exclude the divergence. Next, we solve a collection of three exemplars of Eqs. (5) in backward time along the same trajectory to get three vectors $\{\mathbf{b}(t), \mathbf{c}(t), \mathbf{d}(t)\}$. To avoid dominance of one vector and divergence, we use the Gram-Schmidt orthogonalization and normalization of the vectors in a course of the integration.

At each point of the stroboscopic section $t_n = nT$ the vector $\mathbf{a}_n = \mathbf{a}(nT)$ determines an unstable direction, and all possible linear combinations of $\{\mathbf{b}_n, \mathbf{c}_n, \mathbf{d}_n\} = \{\mathbf{b}(nT), \mathbf{c}(nT), \mathbf{d}(nT)\}$ define a 3D stable subspace of perturbation vectors for the Poincaré map.

To estimate an angle α between the stable and unstable subspaces we first construct a vector $\mathbf{v}_n(t)$ orthogonal to the 3D stable subspace, with components determined from a

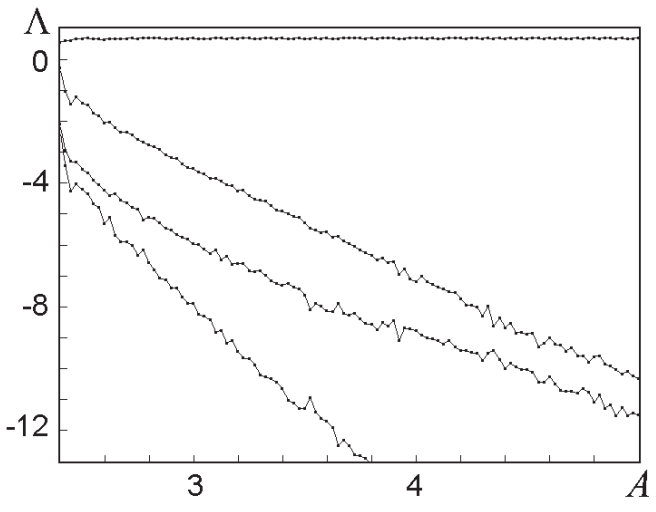

FIG. 2. Computed Lyapunov exponents of the stroboscopic map versus parameter A at $\omega_0 = 2\pi$, $N = T = 10$, and $\varepsilon = 0.5$. Observe that the largest exponent remains almost constant in the whole interval of hyperbolicity being in good agreement with the estimate $\Lambda_1 \approx \log 2$. The left edge of the diagram corresponds to violation of the hyperbolicity.

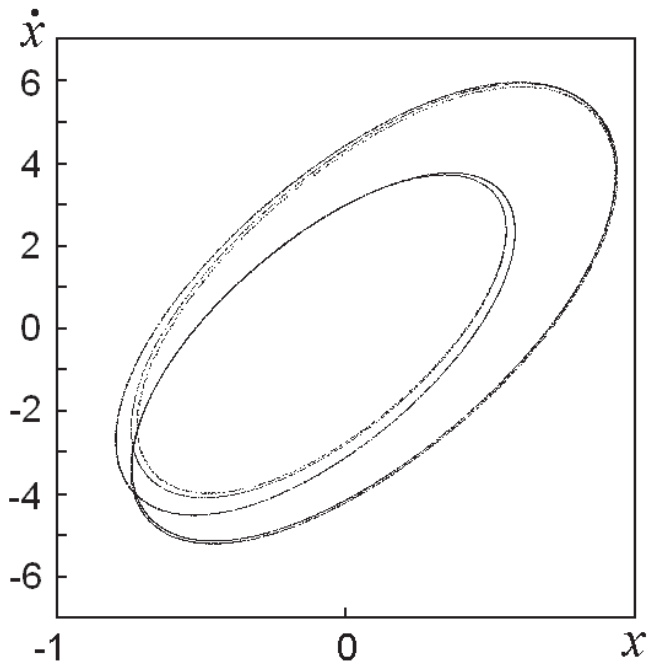

FIG. 3. A portrait of the strange attractor in the stroboscopic Poincaré section in projection onto the plane $(x, \dot{x})$ at $\omega_0 = 2\pi$, $T = N = 4$, $A = 8$, and $\varepsilon = 0.5$.

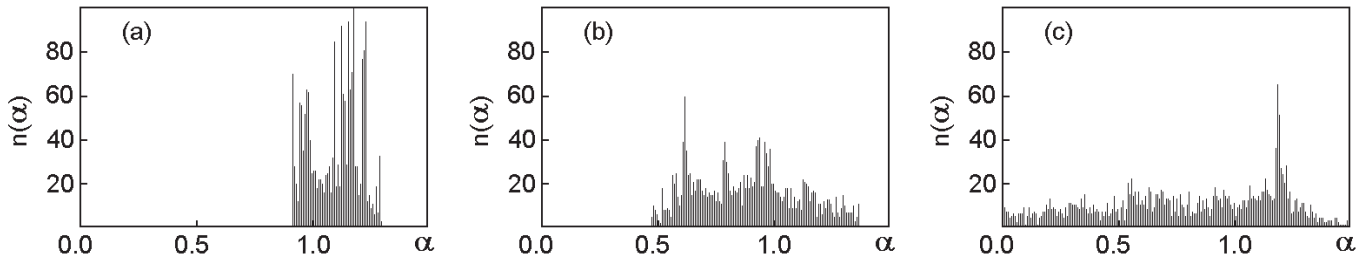

FIG. 4. Histograms for distributions of angles α_n between the stable and unstable subspaces obtained from computational procedures described in the text at $\omega_0 = 2\pi$ and $\varepsilon = 0.5$. Panels (a) and (b) correspond to hyperbolic attractors, respectively, at $N = 10$, $A = 3$ and $N = 4$, $A = 8$, and panel (c) to a nonhyperbolic attractor at $N = 10$, $A = 2.35$.

set of linear equations $\mathbf{v}_n(t) \cdot \mathbf{b}_n(t) = 0$, $\mathbf{v}_n(t) \cdot \mathbf{c}_n(t) = 0$, $\mathbf{v}_n(t) \cdot \mathbf{d}_n(t) = 0$. Then, we compute an angle $\beta_n \in [0, \pi/2]$ between the vectors $\mathbf{v}_n(t)$ and $\mathbf{a}_n(t)$: $\cos\beta_n = |\mathbf{v}_n(t) \cdot \mathbf{a}_n(t)|/|\mathbf{v}_n(t)||\mathbf{a}_n(t)|$ and set $\alpha_n = \pi/2 - \beta_n$. Figure 4 shows histograms for the angles α_n obtained from computations. Diagrams (a) and (b) correspond to the above-mentioned parameter values and demonstrate clearly separation of the distributions from zero α's: the test confirms the hyperbolicity. For comparison, in panel (c) I present a histogram for a nonhyperbolic attractor (that corresponds to the left edge of the plot in Fig. 3, where the exponent Λ_1 becomes notably distinct from log2).

In conclusion, it is worth mentioning again that the present example of a system with hyperbolic strange attractors due to its simplicity may be realized as a physical device, e.g., on a basis of two interacting electronic oscillators. Departing from this system, one can easily construct many other examples of systems with hyperbolic attractors, exploiting the property of structural stability: any small variation of the terms in the equations will not destroy the hyperbolicity. It opens an opportunity for experimental studies of hyperbolic chaos and its features predicted by the mathematical hyperbolic theory (robustness, continuity of the invariant measure, insensitivity of statistical characteristics of the motions in respect to noise, etc.). In addition, it makes conclusive a comparative examination of dynamics of hyperbolic and nonhyperbolic systems of different physical nature.

The author thanks V. S. Afraimovich, V. S. Anishchenko, B. P. Bezruchko, R. S. MacKay, L. A. Mel'nikov, A. S. Pikovsky, and M. G. Rosenblum for discussion and helpful comments. The work was performed under support of RFBR (Grant No. 03-02-16192) and from Research Educational Center of Saratov University (REC-006).

[1] A. Katok and B. Hasselblatt, *Introduction to the Modern Theory of Dynamical Systems* (Cambridge University Press, Cambridge, 1995).

[2] V. Afraimovich and S.-B. Hsu, *Lectures on Chaotic Dynamical Systems*, AMS/IP Studies in Advanced Mathematics Vol. 28 (AMS International Press, Providence, 2003).

[3] R. L. Devaney, *An Introduction to Chaotic Dynamical Systems* (Addison-Wesley, New York, 1989).

[4] E. Ott, *Chaos in Dynamical Systems* (Cambridge University Press, Cambridge, 1993), 2nd ed..

[5] Yu. A. Kuznetsov, *Elements of Applied Bifurcation Theory* (Springer, New York, Berlin, Heidelberg, 1998).

[6] S. E. Newhouse, Publ. Math., Inst. Hautes Étud. Sci. **50**, 101 (1979); V. S. Afraimovich and L. P. Shil'nikov, in *Nonlinear Dynamics and Turbulence*, edited by G. I. Barenblatt, G. Ioss, and D. D. Joseph (Pitman, Boston, London, Melbourne, 1983), Vol. 1.

[7] V. S. Anishchenko, V. V. Astakhov, A. B. Neiman, T. E. Vadivasova, and L. Schimansky-Geier, *Nonlinear Dynamics of Chaotic and Stochastic Systems* (Springer, Berlin, Heidelberg, 2002).

[8] V. S. Afraimovich, V. V. Bykov, and L. P. Shil'nikov, Dokl. Akad. Nauk SSSR **234**, 336 (1977) [Sov. Phys. Dokl. **22**, 253 (1977)].

[9] K. Mischaikow and M. Mrozek, Bull. Am. Math. Soc. **32**, 66 (1995); K. Mischaikow and M. Mrozek, Math. Comput. **67**, 1023 (1998); K. Mischaikow, M. Mrozek, and A. Szymczak, J. Diff. Equ. **169**, 17 (2001).

[10] T. J. Hunt and R. S. MacKay, Nonlinearity **16**, 1499 (2003).

[11] T. J. Hunt, Ph.D. thesis, University of Cambridge, 2000.

[12] V. Belykh, I. Belykh, and E. Mosekilde, Int. J. Bifurcation Chaos Appl. Sci. Eng. (to be published).

[13] S. P. Kuznetsov and Y. P. Seleznev (to be published).

[14] G. Benettin, L. Galgani, A. Giorgilli, and J. M. Strelcyn, Meccanica **15**, 9 (1980).

[15] F. Christiansen and H. H. Rugh, Nonlinearity **10**, 1063 (1997).

[16] H. G. Schuster, *Deterministic Chaos: An Introduction* (Physik Verlag, Weinheim, 1984).

[17] P. Grassberger and I. Procaccia, Physica (Amsterdam) **9D**, 189 (1983).

[18] Y.-C. Lai, C. Grebogi, J. A. Yorke, and I. Kan, Nonlinearity **6**, 779 (1993).

[19] V. S. Anishchenko, A. S. Kopeikin, J. Kurths, T. E. Vadivasova, and G. I. Strelkova, Phys. Lett. A **270**, 301 (2000).